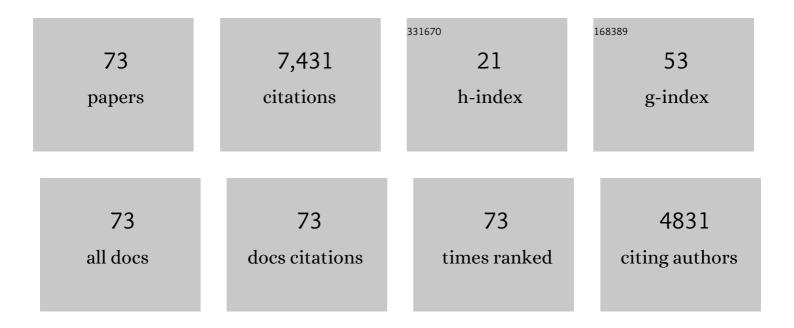


List of Publications by Year in descending order

Source: https://exaly.com/author-pdf/5485877/publications.pdf Version: 2024-02-01



VANC

#	Article	IF	CITATIONS
1	Terabit free-space data transmission employing orbital angular momentum multiplexing. Nature Photonics, 2012, 6, 488-496.	31.4	3,471
2	Terabit-Scale Orbital Angular Momentum Mode Division Multiplexing in Fibers. Science, 2013, 340, 1545-1548.	12.6	2,330
3	Mode Properties and Propagation Effects of Optical Orbital Angular Momentum (OAM) Modes in a Ring Fiber. IEEE Photonics Journal, 2012, 4, 535-543.	2.0	180
4	Highly birefringent elliptical-hole photonic crystal fiber with squeezed hexagonal lattice. Optics Letters, 2007, 32, 469.	3.3	177
5	Silicon waveguide with four zero-dispersion wavelengths and its application in on-chip octave-spanning supercontinuum generation. Optics Express, 2012, 20, 1685.	3.4	156
6	Flattened dispersion in silicon slot waveguides. Optics Express, 2010, 18, 20529.	3.4	137
7	Octave-spanning supercontinuum generation of vortices in an As_2S_3 ring photonic crystal fiber. Optics Letters, 2012, 37, 1889.	3.3	111
8	Flat and low dispersion in highly nonlinear slot waveguides. Optics Express, 2010, 18, 13187.	3.4	91
9	Silicon-on-insulator polarization splitter using two horizontally slotted waveguides. Optics Letters, 2010, 35, 1364.	3.3	71
10	On-chip two-octave supercontinuum generation by enhancing self-steepening of optical pulses. Optics Express, 2011, 19, 11584.	3.4	70
11	Highly dispersive slot waveguides. Optics Express, 2009, 17, 7095.	3.4	53
12	Generation of Orbital Angular Momentum Modes Using Fiber Systems. Applied Sciences (Switzerland), 2019, 9, 1033.	2.5	39
13	Silicon-on-Nitride Waveguide With Ultralow Dispersion Over an Octave-Spanning Mid-Infrared Wavelength Range. IEEE Photonics Journal, 2012, 4, 126-132.	2.0	34
14	On-Chip Octave-Spanning Supercontinuum in Nanostructured Silicon Waveguides Using Ultralow Pulse Energy. IEEE Journal of Selected Topics in Quantum Electronics, 2012, 18, 1799-1806.	2.9	33
15	Orbital Angular Momentum (OAM) Carried by Asymmetric Vortex Beams for Wireless Communications: Theory, Experiment and Current Challenges. IEEE Journal of Selected Topics in Quantum Electronics, 2021, 27, 1-10.	2.9	33
16	Low loss hollow-core waveguide on a silicon substrate. Nanophotonics, 2012, 1, 23-29.	6.0	31
17	Increased bandwidth with flattened and low dispersion in a horizontal double-slot silicon waveguide. Journal of the Optical Society of America B: Optical Physics, 2015, 32, 26.	2.1	30
18	Highly Birefringent Elliptical-Hole Photonic Crystal Fiber With Two Big Circular Air Holes Adjacent to the Core. IEEE Photonics Technology Letters, 2006, 18, 2638-2640.	2.5	27

Yang

#	Article	IF	CITATIONS
19	A Review: Point Cloud-Based 3D Human Joints Estimation. Sensors, 2021, 21, 1684.	3.8	26
20	Air-Core Ring Fiber With >1000 Radially Fundamental OAM Modes Across O, E, S, C, and L Bands. IEEE Access, 2020, 8, 68280-68287.	4.2	23
21	Higher-order-mode assisted silicon-on-insulator 90 degree polarization rotator. Optics Express, 2009, 17, 20694.	3.4	21
22	UWB monocycle pulse generation using two-photon absorption in a silicon waveguide. Optics Letters, 2012, 37, 551.	3.3	21
23	Enabling Technology in High-Baud-Rate Coherent Optical Communication Systems. IEEE Access, 2020, 8, 111318-111329.	4.2	20
24	Ultrasensitive Fabry–Perot Strain Sensor Based on Vernier Effect and Tapered FBC-in-Hollow Silica Tube. IEEE Sensors Journal, 2021, 21, 3035-3041.	4.7	20
25	Highly efficient nonlinearity reduction in silicon-on-insulator waveguides using vertical slots. Optics Express, 2010, 18, 22061.	3.4	18
26	1.6-Octave Coherent OAM Supercontinuum Generation in As ₂ S ₃ Photonic Crystal Fiber. IEEE Access, 2020, 8, 168177-168185.	4.2	18
27	Eye Diagram Measurement-Based Joint Modulation Format, OSNR, ROF, and Skew Monitoring of Coherent Channel Using Deep Learning. Journal of Lightwave Technology, 2019, 37, 5907-5913.	4.6	16
28	Beyond Two-Octave Coherent OAM Supercontinuum Generation in Air-Core As ₂ S ₃ Ring Fiber. IEEE Access, 2020, 8, 96543-96549.	4.2	16
29	Two-Octave Supercontinuum Generation of High-Order OAM Modes in Air-Core Asâ,,Sâ,ƒ Ring Fiber. IEEE Access, 2020, 8, 114135-114142.	4.2	15
30	Solid-State Photonics-Based Lidar With Large Beam-Steering Angle by Seamlessly Merging Two Orthogonally Polarized Beams. IEEE Journal of Selected Topics in Quantum Electronics, 2021, 27, 1-8.	2.9	15
31	Three-Octave Supercontinuum Generation Using SiO ₂ Cladded Si ₃ N ₄ Slot Waveguide With All-Normal Dispersion. Journal of Lightwave Technology, 2020, 38, 3431-3438.	4.6	14
32	Highly dispersive coupled ring-core fiber for orbital angular momentum modes. Applied Physics Letters, 2020, 117, .	3.3	13
33	Detecting Object Open Angle and Direction Using Machine Learning. IEEE Access, 2020, 8, 12300-12306.	4.2	10
34	Analysis of real-time spectral interference using a deep neural network to reconstruct multi-soliton dynamics in mode-locked lasers. APL Photonics, 2020, 5, .	5.7	9
35	Hollow Ring-Core Photonic Crystal Fiber With >500 OAM Modes Over 360-nm Communications Bandwidth. IEEE Access, 2021, 9, 66999-67005.	4.2	9
36	Non-zero dispersion-shifted ring fiber for the orbital angular momentum mode. Optics Express, 2021, 29, 25428.	3.4	8

Yang

#	Article	IF	CITATIONS
37	Multi-Ring-Air-Core Fiber Supporting Numerous Radially Fundamental OAM Modes. Journal of Lightwave Technology, 2022, 40, 4420-4428.	4.6	8
38	3D Joints Estimation of the Human Body in Single-Frame Point Cloud. IEEE Access, 2020, 8, 178900-178908.	4.2	6
39	Polarization Beam Splitter Based on Si3N4/SiO2 Horizontal Slot Waveguides for On-Chip High-Power Applications. Sensors, 2020, 20, 2862.	3.8	6
40	Highly Dispersive Germanium-Doped Coupled Ring-Core Fiber for Vortex Modes. Journal of Lightwave Technology, 2022, 40, 2144-2150.	4.6	6
41	Reconfigurable Multifunctional Operation Using Optical Injection-Locked Vertical-Cavity Surface-Emitting Lasers. Journal of Lightwave Technology, 2009, 27, 2958-2963.	4.6	4
42	Comparing Performance of Deep Convolution Networks in Reconstructing Soliton Molecules Dynamics from Real-Time Spectral Interference. Photonics, 2021, 8, 51.	2.0	4
43	Space division multiplexing technology based on transverse wavenumber of Lommel–Gaussian beam. Optics Communications, 2021, 488, 126835.	2.1	4
44	A Low-Cost High-Resolution Solid-State Lidar With Wavelength Division Multiplexed Components and Interleaved Orthogonal Polarization Grating Couplers. Journal of Lightwave Technology, 2022, 40, 2072-2079.	4.6	4
45	Special Issue on Novel Insights into Orbital Angular Momentum Beams: From Fundamentals, Devices to Applications. Applied Sciences (Switzerland), 2019, 9, 2600.	2.5	3
46	Ultra-Compact Optical Thermo-Hygrometer Based on Bilayer Micro-Cap on Fiber Facet. IEEE Photonics Technology Letters, 2020, 32, 1089-1092.		3
47	Air-Core Ring Fiber Guiding >400 Radially Fundamental OAM Modes Across S + C + L Bands. IEEE Access, 2021, 9, 75617-75625.	4.2	3
48	Proposal for All-Solid Photonic Bandgap Fiber With Improved Dispersion Characteristics. IEEE Photonics Technology Letters, 2007, 19, 1239-1241.	2.5	2
49	Demonstration of 100-Gbit/s DQPSK data exchange between two different wavelength channels using parametric depletion in a highly nonlinear fiber. , 2010, , .		2
50	Air-Core Non-Zero Dispersion-Shifted Fiber With High-Index Ring for OAM Mode. IEEE Access, 2021, 9, 107804-107811.	4.2	2
51	Triple Coupled Ring ore Fiber with Dual Highly Dispersive Windows for Orbital Angular Momentum Mode. Advanced Photonics Research, 2022, 3, .	3.6	2
52	Special Issue on Enabling Technology in Optical Fiber Communications: From Device, System to Networking. Sensors, 2021, 21, 1969.	3.8	1
53	Hollow Ring-Core Hybrid Photonic Crystal Fiber Supporting >500 OAM Modes Across O, E, S, C, L Bands. , 2020, , .		1
54	Solid-State Lidar with Wide Steering Angle Using Counter-Propagating Beams. , 2021, , .		1

Yang

#	Article	IF	CITATIONS
55	Low-Cost Solid-State Lidar with Wide Angle of View Using Wavelength Division Multiplexed Laser Array. , 2021, , .		1
56	3D joints estimation of human body using part segmentation. Information Sciences, 2022, 603, 1-15.	6.9	1
5 7	1.3-Octave Coherent Supercontinuum Generation of OAM Mode in Ring-Core Fiber With All-Normal Dispersion. IEEE Access, 2022, 10, 76990-76997.	4.2	1
58	Tapped delay-line matched filtering using a high-contrast grating hollow-core waveguide. , 2011, , .		0
59	Object Wedge Angle and Direction Identification Using Machine Learning Algorithms. , 2019, , .		0
60	Special Issue on Advanced DSP Techniques for High-Capacity and Energy-Efficient Optical Fiber Communications. Applied Sciences (Switzerland), 2019, 9, 4470.	2.5	0
61	Octave-Spanning Dispersive Slot Waveguide Based Chip-Level Ultrashort Pulse Stretcher. IEEE Access, 2020, 8, 172086-172095.	4.2	0
62	Special Issue on Optical Communications and Networking: Prospects in Industrial Applications. Applied Sciences (Switzerland), 2020, 10, 411.	2.5	0
63	Transition between optical turbulence and dissipative solitons in a complex Ginzburg-Landau equation with quasi-cw noise. Physical Review A, 2021, 103, .	2.5	0
64	7-Ring-Air-Core Trench-Assisted Fibre Supporting >300 Radially Fundamental OAM Modes Across S+C+L Bands. , 2021, , .		0
65	Dispersion Compensating Ring Fibre in the C-Band for OAM Mode. , 2021, , .		0
66	37-Air-Core Chalcogenide Ring Fiber with >4000 Radially Fundamental OAM Modes Across C+L Bands. , 2021, , .		0
67	Beyond Two-Octave OAM Supercontinuum Generation in Gemanium-Doped Ring-Core Fiber. , 2021, , .		0
68	Two-Octave Supercontinuum Generation of OAM Modes in Ring Fiber. , 2021, , .		0
69	19-Ring-Core Chalcogenide Fiber Supporting >2000 Radially Fundamental OAM Modes Across C and L Bands. , 2020, , .		0
70	7-Air-Core-Ring Fiber Supporting > 400 Radially Fundamental OAM Modes Across C and L Bands. , 2020, ,		0
71	Beyond Octave-Spanning Supercontinuum Generation of Optical Vortices in Ring-Core Photonic Crystal Fiber. , 2021, , .		0

5

Y.	A	N	G	

#	Article	IF	CITATIONS
73	Soliton-Induced Mid-Infrared Dispersive Wave in Horizontally-Slotted Siâ,∱Nâ,,, Waveguide. IEEE Access, 2022, 10, 62322-62329.	4.2	Ο